British Journal of Environment & Climate Change

7(3): 182-194, 2017; Article no.BJECC.2017.014
ISSN: 2231–4784

Modeling of Areal Coverage of Snow of an Ungauged Catchment with ArcSWAT

Syeedah Raazia[1,2*] and Showkat Rasool[3]

[1]Department of Civil Engineering, Indian Institute of Technology Delhi, New Delhi, 110016, India.
[2]Department of Civil Engineering, National Institute of Technology Srinagar, J & K, 190011, India.
[3]Department of Agricultural and Food Engineering, Indian Institute of Technology Kharagpur, West Bengal, 721301, India.

Authors' contributions

This work was carried out in collaboration between both authors. Author Syeedah Raazia designed the study, obtained and prepared the data for the model, carried out the simulation modeling and wrote the first draft of the manuscript. Author Showkat Rasool managed the literature searches, obtained the satellite imagery and performed the mapping task for the study. Both authors performed the image classification tasks and the analysis and interpretation of the results. Both authors read and approved the final manuscript.

Article Information

DOI: 10.9734/BJECC/2017/36139

Received 4th July 2017
Accepted 19th September 2017
Published 27th September 2017

Original Research Article

ABSTRACT

Aim: The study aimed at modeling the aerial extent of snow cover of an ungauged mountainous Himalayan region using the temperature index-based method of ArcSWAT model.
Study Design: 20 year precipitation and temperature data along with elevation information were used in the simulation of accumulated snow.
Place and Duration of Study: Department of Civil Engineering, Indian Institute of Technology Delhi, India from January 2014 to June 2014.
Methodology: The basin was divided into 3 elevation bands and daily snow accumulation depths were obtained for each of the elevation zones. To account for the lack of measured snow depths, satellite imagery was used to calibrate the model. LandsatLook imagery taken on different dates in a year was visually interpreted for the presence of snow cover in the different elevation zones. In addition, image classification was used to identify snow covered region in each elevation band and to determine the percent area under snow cover. Temperature and precipitation lapse rates were alternately adjusted till the simulated results were in agreement with the results obtained from the imagery. Simulation was deemed to be acceptable whenever a non-zero snow depth was simulated by the ArcSWAT model for above 5 percent area under snow determined from the satellite imagery.

**Corresponding author: E-mail: raazia_42phd15@nitsri.net;*

Results: Calibration resulted in a temperature lapse rate of -6°C/km and a precipitation lapse rate of 5mm/km for the region. Snow accumulation depths obtained from the calibrated model for all elevation zones agreed reasonably well with the results obtained from image classification.
Conclusion: ArcSWAT could be suitably used to model the snow cover of ungauged hilly catchments. Satellite imagery/remote sensing data can be a suitable aid to calibrate the snow model for ungauged regions. Division into greater number of elevation zones is expected to improve the calibration process.

Keywords: Snow modeling; snow coverage; orographic variation; elevation bands; ArcSWAT; Himalayan catchment.

1. INTRODUCTION

Snow is an essential component of hydrological water balance in cold regions. It greatly affects the hydrological behaviour of regions where a significant proportion of precipitation is in the form of snow and/or a large area of land remains under snow for a considerable part of the year. Occurrence of precipitation in the form of snow affects its redistribution. Snow neither contributes to immediate surface runoff, nor does it percolate down the soil or recharge the groundwater within the same temporal scale as rain. Moreover, the presence of snow cover on the land surface also alters the catchment behaviour towards generating a hydrological response to other forms of precipitation as snowpack essentially presents a modified land cover to the incoming precipitation. Relevant snowpack parameters essential for accurate modeling of catchment hydrology of snowy regions include the areal extent and depth of the snow pack, density of the snow pack and temperature of the snow pack. Snowpack equates to a water reservoir. Temperature of the snowpack affects its melting rate and thus its contribution to surface and subsurface flows. The amount of snowmelt depends upon its depth and aerial extent. Snow is a porous medium. Accumulated snow acts as a secondary storage medium to the incoming precipitation as it allows for the infiltration of precipitation occurring as rain. This feature depends on depth, aerial extent and density of the snow pack.

Snow accumulation and melting is conventionally modeled using either conceptual (temperature index-based) models [1,2,3] or physical (energy balance) models [4,5,6,7,8,9,10]. Energy balance models simulate the physical processes affecting the energy content of the snowpack. These are based on the assessment of energy fluxes to and from the surface of the snow pack [11]. Point models of energy balance assess the energy budget at one location [12,13] whereas the distributed models estimate energy budget over an area [14,15]. These models use a multitude of meteorological variables (net radiation, global radiation, albedo, long wave radiation, turbulent and other heat fluxes) as input to quantify sensible heat, latent heat and ground heat fluxes. On the other hand, conceptual models such as SWAT relate snow melting and accumulation to readily available data such as air temperature and precipitation [16]. These models are based on temperature index method for calculation of snowmelt, in which, above a threshold or melt temperature, the amount of snowmelt on any day is a function of the temperature on that day. Studies have shown that temperature-based snowmelt models perform equally well as energy balance snowmelt models under most conditions, in addition to being simpler models [17,18,19]. The success of temperature index models is attributed to the high correlation of temperature with energy balance components [18]. Temperature index-based models are widely used in flood forecasting and runoff modelling [20], glacier mass balance modelling [21] and in modelling response of snow and ice under climate change scenarios [22]. Many researchers have evaluated the performance of conceptual snow process models using either measured snow depth or stream flow data [3,23,24]. Remote sensing data has also been used together with *in-situ* measurements to validate the performance of snow models [25,26]. The high reflectance of snow makes it differentiable from other land covers in satellite imagery which enables identification of snow covered area. Moreover, satellite data is available at a range of spatial and temporal resolutions making it suitable for mapping of snow cover [27]. Snow covered areas can be identified from satellite imagery by various techniques such as manual delineation [28], using spectral ratios [29,30,31], spectral indices, the most common of which is the Normalized Difference Snow Index (NDSI) [32,33,34] or digital image classification, which can be supervised [35,36] or unsupervised [37].

In the present study, an attempt has been made to model the aerial spread of snow cover over an ungauged catchment using the temperature index-based method of ArcSWAT model, calibrated with the help of snow cover information extracted from satellite imagery by supervised classification technique.

ArcSWAT is the GUI version of the Soil Water Assessment Tool (Texas A & M University) that works within the ArcGIS environment. SWAT classifies precipitation as snow or rain on the basis of average daily temperature (T_{av}) using a user defined threshold temperature ($T_{s\text{-}r}$) below which precipitation is considered as snow. The amount of snow in the snowpack on ground is defined by the mass balance given in Equation 1.

$$SNO = SNO + P_s - E_{sub} - SNO_{melt} \quad (1)$$

SNO is the water equivalent of the snow pack on a given day, P_s is the precipitation in the form of snow, E_{sub} is the water lost from the snow pack by sublimation taken from the evaporation value for the given day at the given location, and SNO_{melt} is the amount of snowmelt on the given day, all in mmH_2O. SWAT uses areal depletion curve [38] to model the variable snow coverage of an area. It correlates growth and recession of snow pack over a region with the amount of snow present in the region as expressed by Equation 2.

$$sno_{cov} = \frac{SNO}{SNO_{100}}\left(\frac{SNO}{SNO_{100}} + exp\left(cov_1 - cov_2\frac{SNO}{SNO_{100}}\right)\right)^{-1} \quad (2)$$

where sno_{cov} is the snow covered fraction of an area, SNO_{100} is the threshold snow depth above which 100 per cent of the area is covered with snow, cov_1 and cov_2 are coefficients defining the slope of the areal depletion curve. Snow melt (SNO_{melt}) in Equation 1 is modeled as a linear function of difference between arithmetic mean of maximum air temperature (T_{mx}, °C) and snow pack temperature (T_{snow}, °C) and the temperature at which the snow melts (T_{mlt}, °C). The amount of snow melt generated depends on the areal coverage of snow and the melt factor (b_{mlt}, mmH_2O/day-°C) of the region (Equation 3).

$$SNO_{mlt} = b_{mlt} sno_{cov}\left(\frac{T_{snow} + T_{mx}}{2} - T_{mlt}\right) \quad (3)$$

Temperature in the snow pack on a given day ($T_{snow,d}$, °C) is calculated as a function of mean of the snow pack temperature in the preceding days ($T_{snow,d-1}$, °C) and the air temperature in which the influence of each is controlled by means of a lagging factor (l_{sno}) as given in equation 4.

$$T_{snow,d} = T_{snow,d-1}(1 - l_{sno}) + T_{av}.l_{sno} \quad (4)$$

The melt factor b_{mlt} is a seasonal factor which is maximum for summer solstice and minimum for winter solstice.

Spatial distribution of snow is affected by a number of factors such as elevation, slope, radiation loading, wind and vegetation cover [39]. Variation in elevation has a strong effect on the spatial variation of snow depth [40,41]. Variability in snow cover due to differences in elevation is far more pronounced than the variability due to other factors [42], especially in mountainous terrain. The most common approach to allow for this variability is to spatially discretize the region into elevation bands. ArcSWAT allows dividing a region into elevation bands to account for orographic variations in temperature and precipitation, thus enabling modeling of elevation effects on the distribution of snow. The gauge values of precipitation and temperature are adjusted to give the values of these variables in any elevation band (P_{band}, mmH_2O and T_{band}, °C) by means of precipitation lapse rate (*plaps*, mmH_2O/km) and temperature lapse rate (*tlaps*, °C/km), respectively (Equations 5 and 6).

$$P_{band} = P_i + \left(EL_{band} - EL_{gage}\right)\frac{plaps}{1000 days_{pcp,yr}} \quad (5)$$

$$T_{band} = T + \left(EL_{band} - EL_{gage}\right)\frac{tlaps}{1000} \quad (6)$$

EL_{band} (m) is the mean elevation of the band and EL_{gage} (m) is the elevation of the rain gauge or the temperature gauge. $days_{pcp.yr}$ is the average number of wet days in a year. Thus, snow accumulation and melting can be obtained for each elevation band separately.

2. STUDY AREA DESCRIPTION

The study area is situated in the Himalayan mountain ranges between 34°5'4.4088" and 34°14'3.624"n latitudes and 74°49'21.094" and 75°9'2.722" e longitudes (Fig. 1). The region has a mountainous relief extending between elevations 1576 and 4360 meters above sea level. The basin having an area of about 250 square kilometers forms a part of the catchment of the world famous Dal Lake in India. It drains into the lake through a number of streams, most of which join a deep, dark channel locally known as the *Telbal Nallah*.

The region has a sub-Mediterranean type of climate with an average annual precipitation of 870 mm. Most of the precipitation occurs from December to March. The mean monthly maximum temperature is 30°C and the mean monthly minimum temperature is -11°C. During winter months, the temperature drops to below freezing point causing precipitation to occur as snow. Thawing starts around February in the lower reaches. However, the upper reaches remain covered with snow for nearly half of the year.

3. METHODOLOGY

In the present study, 20 year precipitation and temperature data for the years 1991 to 2010 recorded at Sher e Kashmir University of Agricultural Sciences and Technology (SKUAST) Kashmir gauging station were used to model daily snow accumulation in the study area. The gauging station is located within the study domain at an elevation of 1606 meter above sea level. The study domain presents a hilly topography with rapidly increasing elevations. Hence the elevation effects on both temperature and precipitation were considered. The region was divided into 3 elevation bands viz. 1576 m to 2504 m (1), 2504 m to 3432 m (2) and 3432 m to 4360 m (3) as shown in Fig. 2.

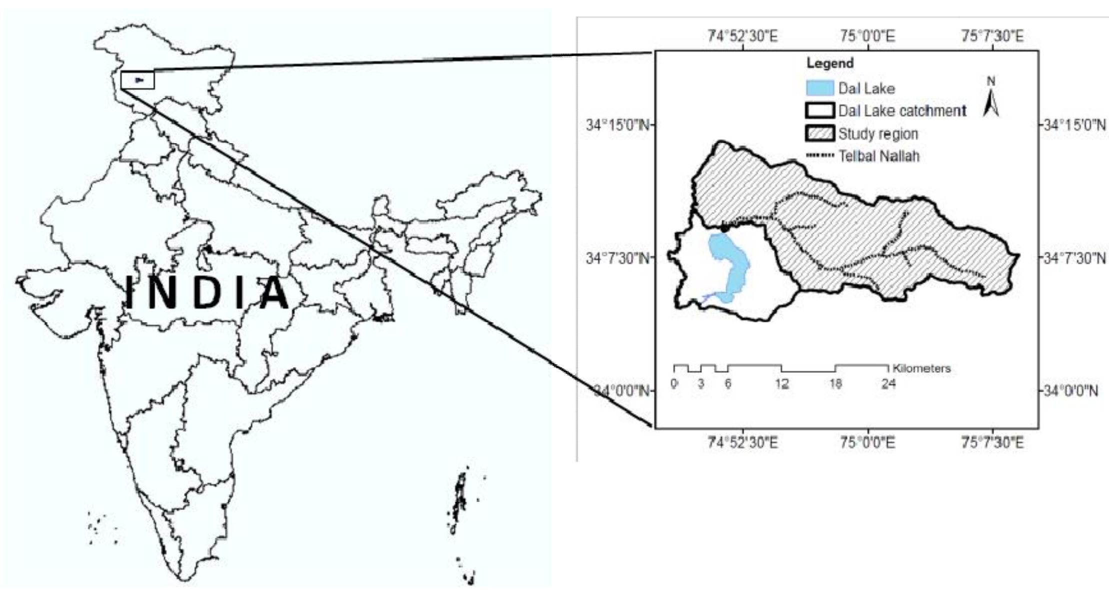

Fig. 1. Study area location

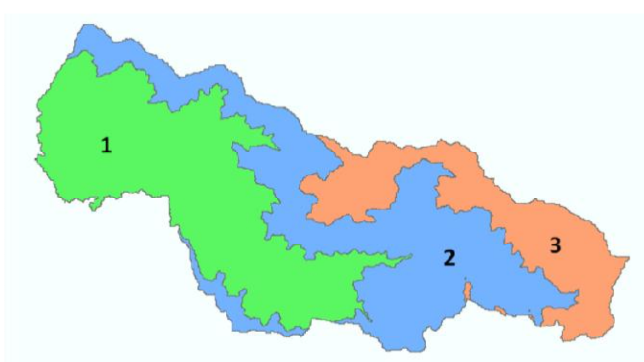

Fig. 2. Division of study region into elevation bands 1. 1576 m to 2504 m 2. 2504 m to 3432 m 3. 3432 m to 4360 m

Initially a precipitation lapse rate of 1 mm/km and temperature lapse rate of -1°C/km were applied. Since the catchment is ungauged, snow depth measurements are not available. Thus, LandsatLook imagery (downloaded from http://landsatlook.usgs.gov/) of the region taken on different dates during the year 2000 was interpreted for areal extent of snow cover. These imagery, as per USGS guidelines are suitable for visual interpretation of land cover. Contours representing 2500 m and 3500 m elevations were generated using 30m x 30m ASTER DEM and overlaid on these imagery so that the regions delineated by these contours would closely correspond to the modeled elevation bands. For each elevation band, presence or absence of snow cover was visually interpreted from the imagery taken on different dates of a year. Image classification technique was used to identify snow in the study domain. The classified image was split into elevation zones defined by the above contours (Fig. 3a, 3b, 3c). For each elevation band, pixel count for snow was compared against the total pixel count to determine the percent area under snow cover.

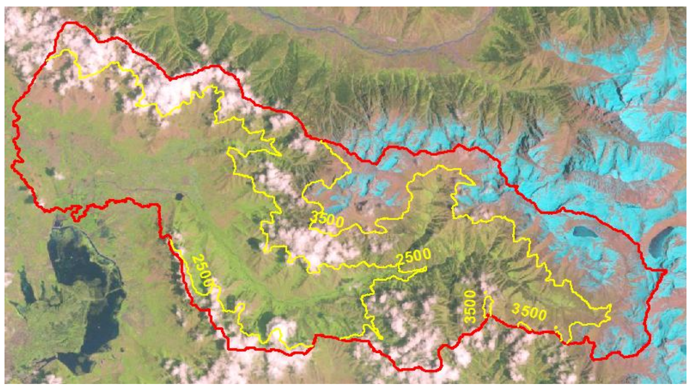

(a)

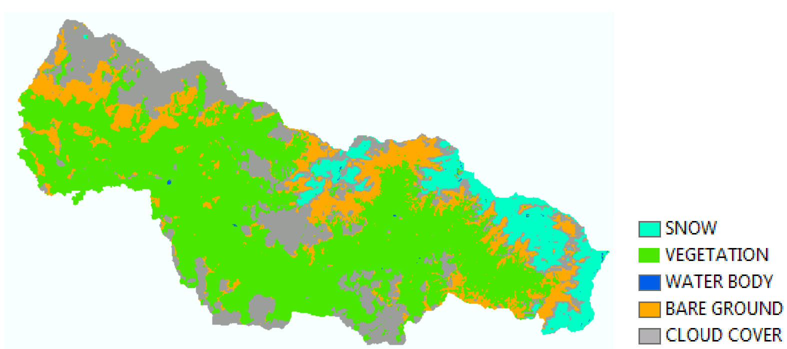

(b)

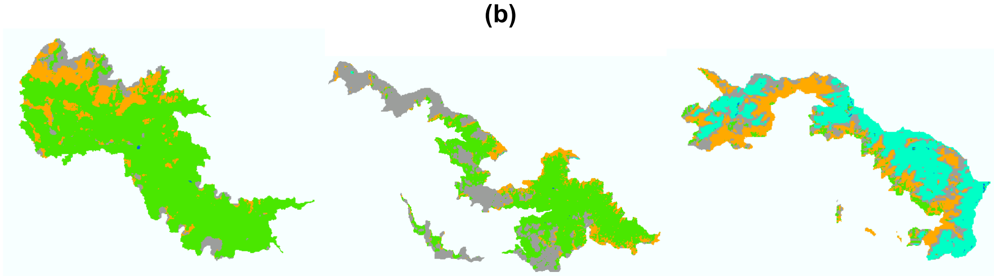

(c)

Fig. 3. Steps in image processing (a) LandsatLook image (b) Classified image clipped to domain (c) Classified image split into elevation zones

Red line is the study domain boundary and yellow lines are 2500 m and 3500 m contours

4. RESULTS AND DISCUSSION

A threshold of 8 percent area under snow in the classified images was used to indicate the presence of snow in any elevation band. Temperature and precipitation lapse rates used by the ArcSWAT model were alternately adjusted till the model results agreed with those interpreted by image processing. Simulation results were considered acceptable whenever the ArcSWAT model resulted in a non-zero snow depth for all the tested instances for which more than 5 percent area under snow was obtained by image classification. The calibrated values for precipitation and temperature lapse rates were respectively chosen to be 5 mm/km and -6°C/km.

Fig. 4(a) shows LandsatLook images of the study domain taken on different dates of the year 2000. According to the guidelines of the USGS, snow cover is represented by light blue color reflection in these images. Fig. 4(b) shows the respective classified images obtained by applying the above guideline in image classification process.

Fig. 5 shows a plot of accumulated snow depths in the 3 elevation bands of the study region over the year 2000 that were obtained using the calibrated ArcSWAT snow model. A summary of the comparison of model simulated occurrence of snow cover and that interpreted from the classification of the LandsatLook imagery for all the 3 elevation bands is given in Table 1. Model prediction was considered to be agreeable for all cases where non-zero snow depth is predicted for area under snow exceeding 8 percent. No conclusions were made for the cases where cloud cover exceeded 30 percent and the visible region showed some snow.

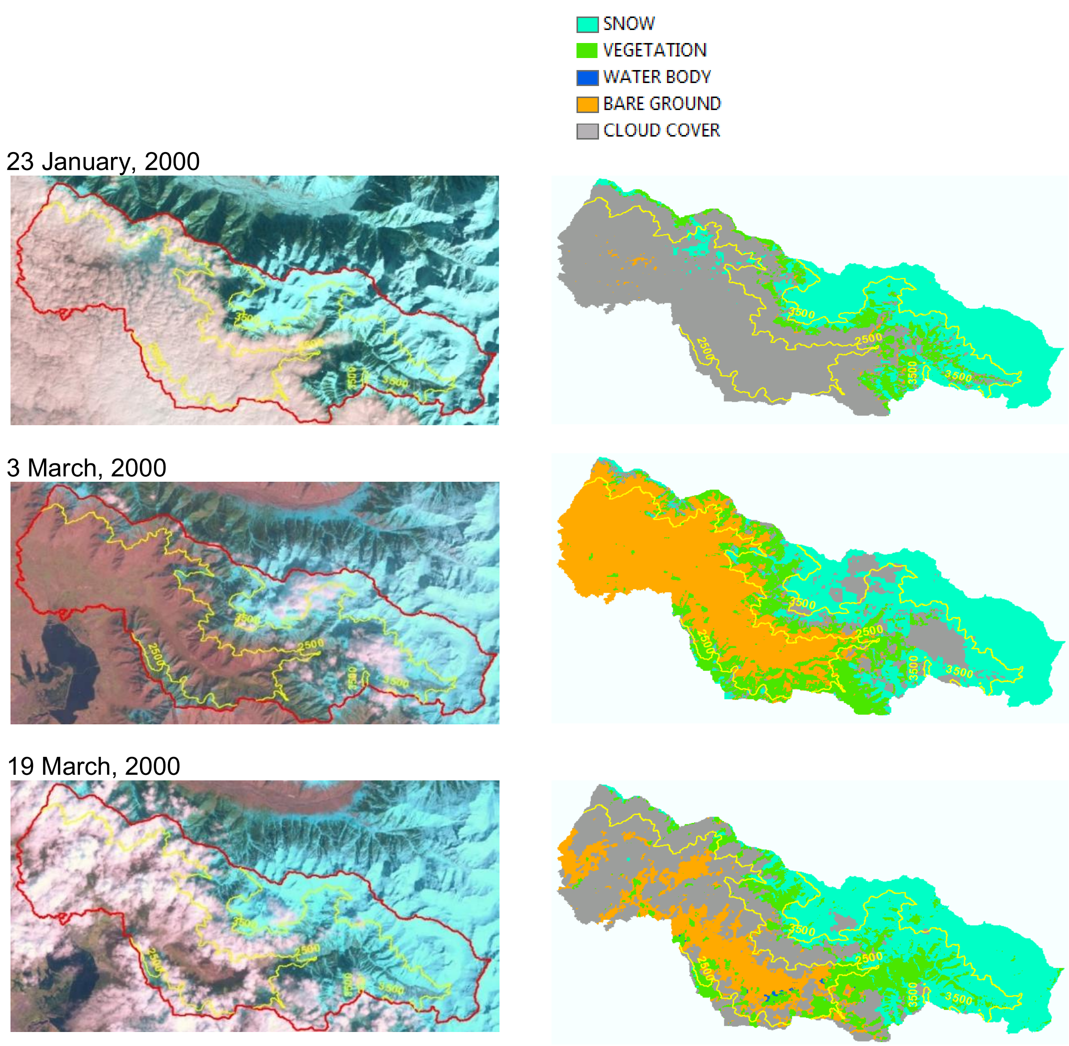

12 April, 2000

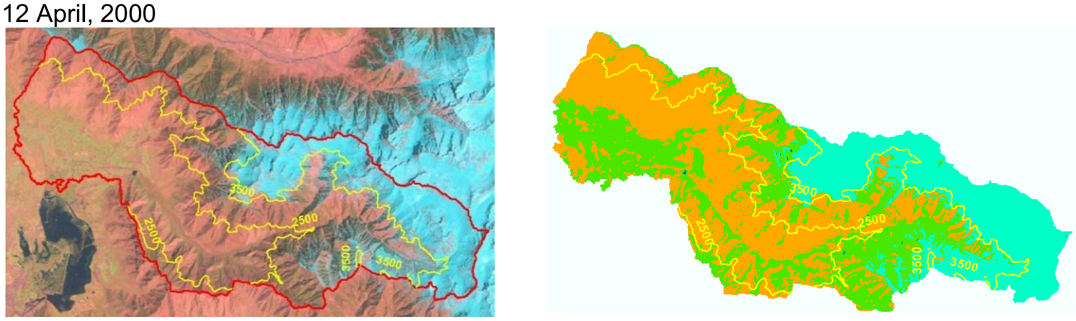

28 April, 2000

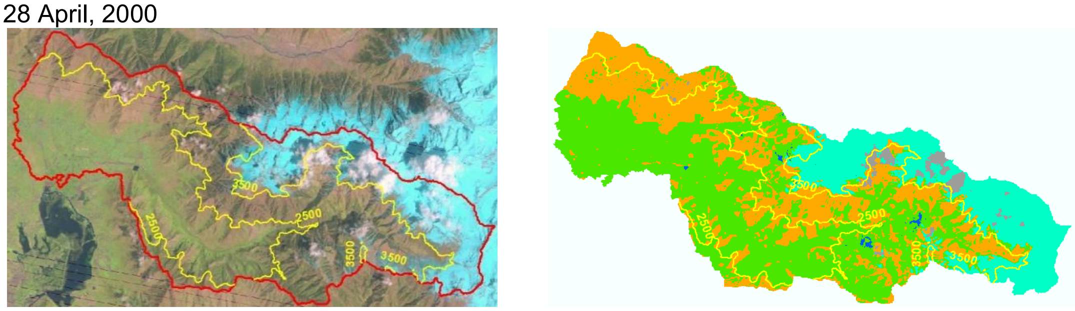

6 May, 2000

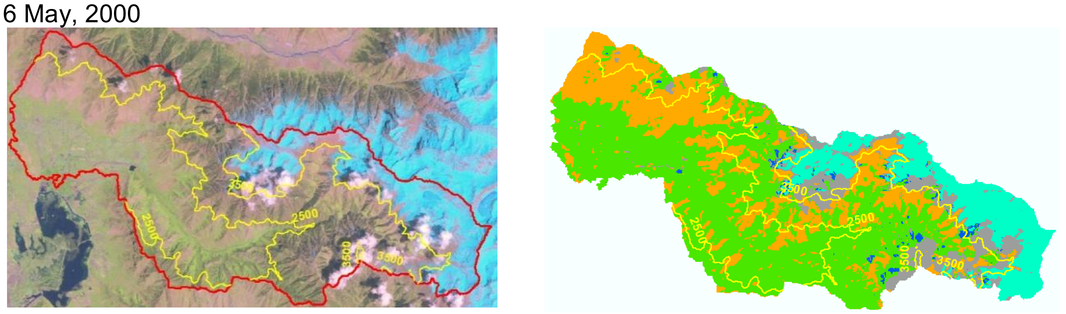

14 May, 2000

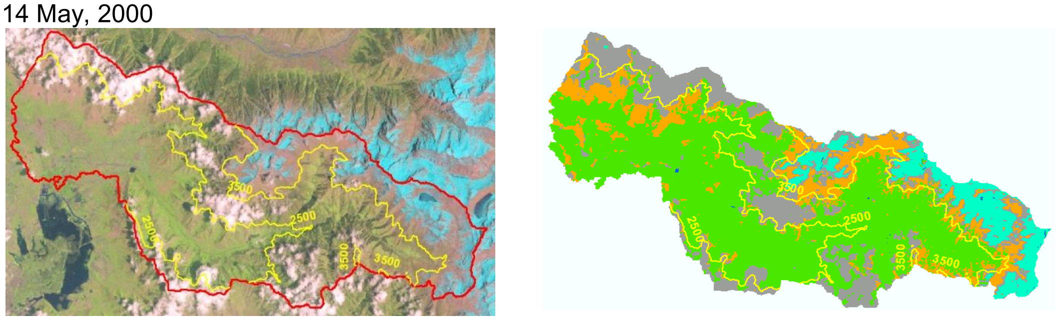

26 August, 2000

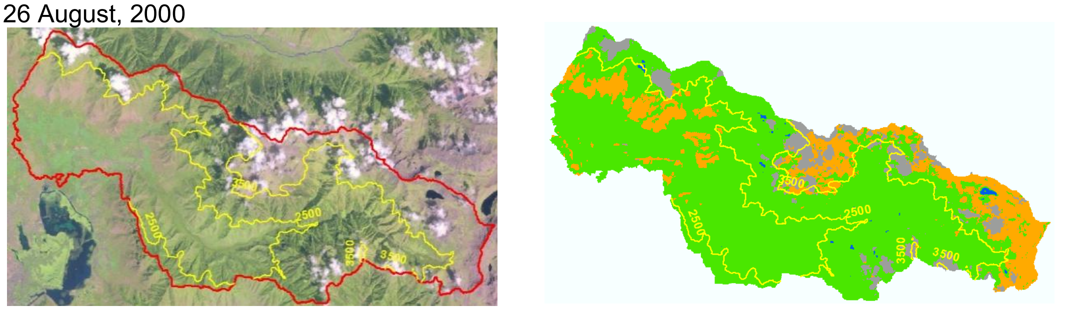

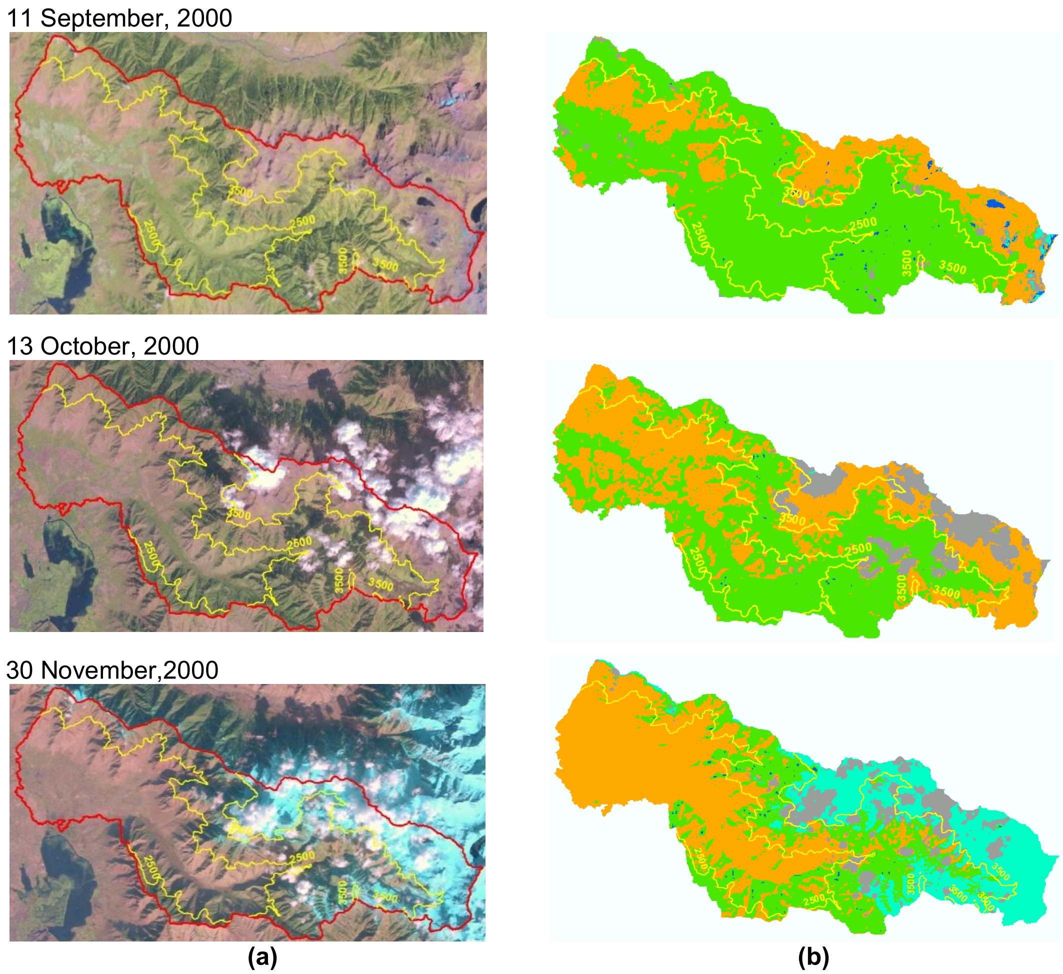

Fig. 4. (a) LandsatLook images and (b) digitally classified images of the study domain
Red line is the study domain boundary and yellow lines are 2500 m and 3500 m contours

Table 1 indicates that the model results after calibration agree with the actual situation in most of the cases, with 2 cases of mismatch and 4 cases where no conclusions could be drawn due to cloud cover, out of a total of 33 tested cases. Thus, it can be inferred that the snow modeling equations of ArcSWAT can be efficiently used with any hydrological model for reliable simulation of hydrological behaviour of an ungauged region.

Fig. 6 shows a plot of accumulated snow depths in the different elevation bands of the study domain for the years 2005 to 2008 obtained at the calibrated values of precipitation and temperature lapse rates. Results indicate that the higher elevation zone of the region of interest which includes mountain peaks remains covered with snow for nearly half of the year, the intermediate zone remains under snow cover for about a quarter of the year whereas in the lower zone, snow is present for a period of 1 to 2 months. This is also true to the natural observations since at low elevations, temperatures are higher than those at higher elevations and precipitation is in lesser amounts and mostly in the form of rain.

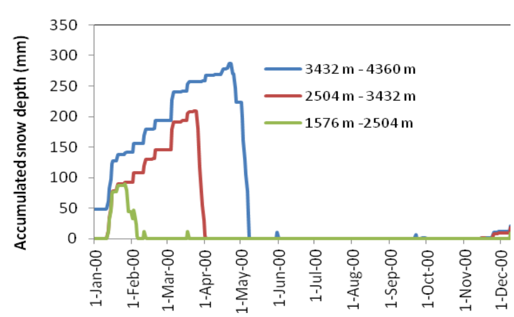

Fig. 5. Snow depth simulated in 3 elevation bands (1576-2504 m, 2504-3432 m, 3432-4360 m) for the year 2000

Table 1. Comparison of model results with classified LandsatLook imagery

Date	Model simulated snow depth	Visual interpretation from imagery	Pixel count of snow	Percent area under snow	Cloud cover (pixels, percent)	Remarks about model performance
	Elevation band			**Total pixels =** 111446		
	1576 m to 2504 m	**Below 2500 m**				
23 Jan, 2000	42 mm	Cloudy, not clear	2881	2.59	107692, 96.63	Uncertain
3 Mar, 2000	Zero	Negligible snow	507	0.45	832, 0.75	Agreeable
19 Mar, 2000	4 mm	Cloudy, snow pockets visible	527	0.47	60145, 53.97	Uncertain
12 Apr, 2000	Zero	No snow	0	0	0,0	Agreeable
28 Apr, 2000	Zero	No snow	0	0	0,0	Agreeable
6 May, 2000	Zero	No snow	0	0	314,0.28	Agreeable
14 May, 2000	Zero	No snow	3	0	8691,7.8	Agreeable
26 Aug, 2000	Zero	No snow	0	0	64,0.06	Agreeable
11 Sep, 2000	Zero	No snow	0	0	683,0.61	Agreeable
13 Oct, 2000	Zero	No snow	1	0	497,0.45	Agreeable
30 Nov,2000	Zero	No snow	0	0	415,0.37	Agreeable
	Elevation band			**Total pixels =** 109021		
	2504 m to 3432 m	**2500 m to 3500 m**				
23 Jan, 2000	82 mm	Little snow in visible region	29122	26.71	56831, 52.13	Uncertain
3 Mar, 2000	140 mm	Partly snow covered	33161	30.42	25273, 23.18	Agreeable
19 Mar, 2000	191 mm	Partly snow covered	37310	34.22	38522, 35.33	Uncertain
12 Apr, 2000	Zero	Very little snow	21012	19.27	0,0	Mismatch
28 Apr, 2000	Zero	Negligible snow	8288	7.60	2150, 1.97	Agreeable
6 May, 2000	Zero	No snow	2200	2.02	12508, 11.47	Agreeable
14 May, 2000	Zero	No snow	106	0	37842, 34.71	Agreeable
26 Aug, 2000	Zero	No snow	0	0	10318, 9.46	Agreeable
11 Sep, 2000	Zero	No snow	0	0	1113, 1.02	Agreeable
13 Oct, 2000	Zero	No snow	0	0	8196, 7.52	Agreeable
30 Nov,2000	16 mm	Little snow	22234	20.39	10349, 9.49	Agreeable
	Elevation band			**Total pixels =** 56607		
	3432 m to 4360 m	**Above 3500 m**				
23 Jan, 2000	142 mm	Full snow cover	56290	99.44	197,0.35	Agreeable
3 Mar, 2000	223 mm	Full snow cover	50431	89.09	6078, 10.74	Agreeable
19 Mar, 2000	254 mm	Full snow cover	53652	94.78	1569, 2.77	Agreeable

Date	Model simulated snow depth	Visual interpretation from imagery	Pixel count of snow	Percent area under snow	Cloud cover (pixels, percent)	Remarks about model performance
12 Apr, 2000	267 mm	Full snow cover	55194	97.50	0,0	Agreeable
28 Apr, 2000	217 mm	Partly snow covered	47728	84.31	3377, 5.97	Agreeable
6 May, 2000	18 mm	Partly snow covered	36925	65.23	14102, 24.91	Agreeable
14 May, 2000	Zero	Little snow	23726	41.91	13649, 24.11	Mismatch
26 Aug, 2000	Zero	No snow	0	0	11528, 20.36	Agreeable
11 Sep, 2000	Zero	Negligible snow	947	1.67	3389, 5.99	Agreeable
13 Oct, 2000	Zero	Negligible snow under cloud cover	59	0.10	20700, 36.56	Agreeable
30 Nov,2000	19 mm	Nearly full snow cover	41579	73.45	13913, 24.58	Agreeable

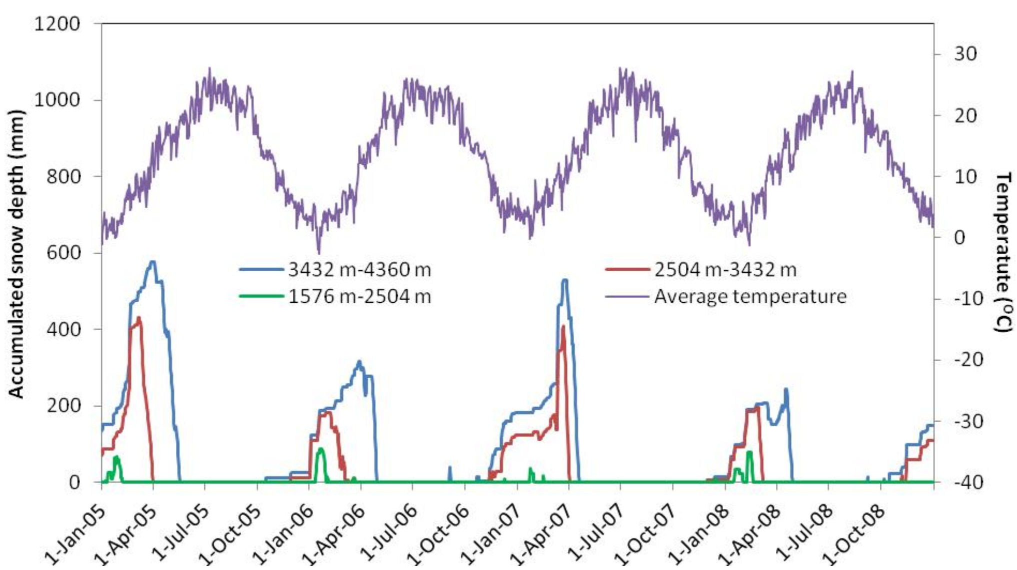

Fig. 6. Accumulated snow depths simulated by calibrated model

5. CONCLUSION

The temperature index-based snow model of ArcSWAT is a simple and efficient tool that can be used with hydrological models to simulate snow accumulation and melting of ungauged regions. The model includes very few parameters that are very easy for interpretation and adjustment. For ungauged regions with hilly topography, division into elevation bands for modeling snow cover is an efficient method which enables to account for the effect of altitude on meteorological variables. Where measured data is lacking, information extracted from satellite imagery can be reliably used to calibrate the model. Complex analysis of remote sensing data to estimate snow depths to aid in calibration may not always be necessary in this regard. Sufficient agreement between reality and simulated results can be obtained by simply comparing the presence or absence of snow in any elevation zone respectively with non-zero or zero accumulated snow depth being simulated by the model. A finer division into greater number of elevation zones is expected to improve model performance as it will allow for a more precise calibration of the model.

The modeling activity revealed that orographic effects are predominant in the study region. Both the temperature and amount of precipitation are significantly dependent on elevation. The amount of precipitation increases with altitude which can also be concluded from the greater depths of accumulated snow at higher elevations. Calibration of the model for temperature and precipitation lapse rates indicates that the temperature in the study region falls by about 6°C for every 1 kilometer rise in elevation, whereas the precipitation increases by nearly 5 mm for the same increase in altitude. As can be inferred from Table 1, not only the areal extent of snow cover but also the depth of accumulated snow shows a strong correlation with elevation, for different seasons.

ACKNOWLEDGEMENTS

The authors are thankful to the Division of Agronomy, SKUAST Kashmir, J&K, India for providing the necessary meteorological data required to run the simulation.

COMPETING INTERESTS

Authors have declared that no competing interests exist.

REFERENCES

1. Verbunt M, Gurtz J, Jasper K, Lang H, Warmerdam P, Zappa M. The hydrological role of snow and glaciers in alpine river basins and their distributed modeling. J. Hydrol. 2003;282(1):36-55.
2. Hock R. Temperature index melt modelling in mountain areas. J. Hydrol. 2003;282(1): 104-15.
3. Formetta G, Kampf SK, David O, Rigon R. Snow water equivalent modeling components in NewAge-JGrass. Geoscientific Model Development. 2014; 7(3):725.
4. Hardy JP, Davis RE, Jordan R, Li X, Woodcock C, Ni W, McKenzie JC. Snow ablation modeling at the stand scale in a boreal jack pine forest. J. Geophy. Res. Atmos. 1997;102(D24):29397-405.
5. Cline DW, Bales RC, Dozier J. Estimating the spatial distribution of snow in mountain basins using remote sensing and energy balance modeling. Water Resour. Res. 1998;34(5):1275-85.
6. Pan M, Sheffield J, Wood EF, Mitchell KE, Houser PR, Schaake JC, Robock A, Lohmann D, Cosgrove B, Duan Q, Luo L. Snow process modeling in the North American Land Data Assimilation System (NLDAS): 2. Evaluation of model simulated snow water equivalent. J. Geophy. Res. Atmos. 2003;108(D22).
7. Garen DC, Marks D. Spatially distributed energy balance snowmelt modelling in a mountainous river basin: Estimation of meteorological inputs and verification of model results. J. Hydrol. 2005;315(1):126-53.
8. Shamir E, Georgakakos KP. Estimating snow depletion curves for American River basins using distributed snow modeling. J. Hydrol. 2007;334(1):162-73.
9. Liston GE, Elder K. A distributed snow-evolution modeling system (SnowModel). J. Hydromet. 2006;7(6):1259-76.
10. Andreadis KM, Storck P, Lettenmaier DP. Modeling snow accumulation and ablation processes in forested environments. Water Resour. Res. 2009;45(5).
11. Hock R. Glacier melt: A review of processes and their modelling. Progress in Physical Geography. 2005;29(3):362-91.
12. Oerlemans J, Reichert BK. Relating glacier mass balance to meteorological data by using a seasonal sensitivity characteristic. J. Glaciology. 2000;46(152):1-6.
13. Konya K, Matsumoto T, Naruse R. Surface heat balance and spatially distributed ablation modelling at Koryto Glacier, Kamchatka peninsula, Russia. Geografiska Annaler: Series A, Physical Geography. 2004;86(4):337-48.
14. Plüss C. The energy balance over an alpine snowcover. Zürcher Geographische Schriften, Department of Geography, ETH Zürich. 1997;65:115.
15. Klok EJ, Oerlemans J. Model study of the spatial distribution of the energy and mass balance of Morteratschgletscher, Switzerland. J. Glaciology. 2002;48(163): 505-18.
16. Franz KJ, Hogue TS, Sorooshian S. Operational snow modeling: Addressing the challenges of an energy balance model for National Weather Service forecasts. J. Hydrol. 2008;360(1):48-66.

17. Hock R. Temperature index melt modelling in mountain areas. J. Hydrol. 2003;282(1): 104-15.
18. Ohmura A. Physical basis for the temperature-based melt index method. J. Appl. Meteorol. 2001;40:753–761.
19. Zappa M, Pos F, Strasser U, Warmerdam P, Gurtz J. Seasonal water balance of an Alpine catchment as evaluated by different methods for spatially distributed snowmelt modelling. Nord. Hydrol. 2003;34(3):179–202.
20. World Meterology Organization (WMO). Intercomparison of models for snowmelt runoff. Operational Hydrology 1986. Report 23 (WMO no. 646).
21. Oerlemans J, Anderson B, Hubbard A, Huybrechts P, Johannesson T, Knap WH, Schmeits M, Stroeven AP, Van de Wal RS, Wallinga J, Zuo Z. Modelling the response of glaciers to climate warming. Climate dynamics. 1998;14(4):267-74.
22. Braithwaite RJ, Zhang Y. Modelling changes in glacier mass balance that may occur as a result of climate changes. Geografiska Annaler: Series A, Physical Geography. 1999;81(4):489-96.
23. Troin M, Caya D. Evaluating the SWAT's snow hydrology over a Northern Quebec watershed. Hydrol. Process. 2014;28(4): 1858-73.
24. Garee K, Chen X, Bao A, Wang Y, Meng F. Hydrological modeling of the Upper Indus Basin: A case study from a High-Altitude Glacierized Catchment Hunza. Water. 2017;9(1):17.
25. Fuka DR, Easton ZM, Brooks ES, Boll J, Steenhuis TS, Walter MT. A simple process-based snowmelt routine to model spatially distributed snow depth and snowmelt in the SWAT model. J. Amer. Water Res. Assoc. 2012;48(6):1151-61.
26. Grusson Y, Sun X, Gascoin S, Sauvage S, Raghavan S, Anctil F, Sáchez-Pérez JM. Assessing the capability of the SWAT model to simulate snow, snow melt and streamflow dynamics over an alpine watershed. J. Hydrol. 2015;531:574-88.
27. Arora MK, Shukla A, Gupta RP. Digital image information extraction techniques for snow cover mapping from remote sensing data. In Encyclopedia of Snow, Ice and Glaciers, Springer Netherlands. 2011;213-232.
28. Khromova TE, Osipova GB, Tsvetkov DG, Dyurgerov MB, Barry RG. Changes in glacier extent in the eastern Pamir, Central Asia, determined from historical data and ASTER imagery. Remote Sensing of Environment. 2006;102(1):24-32.
29. Jacobs JD, Simms ÉL, Simms A. Recession of the southern part of Barnes Ice Cap, Baffin Island, Canada, between 1961 and 1993, determined from digital mapping of Landsat TM. J. Glaciology. 1997;43(143):98-102.
30. Bronge LB, Bronge†* C. Ice and snow-type classification in the Vestfold Hills, East Antarctica, using Landsat-TM data and ground radiometer measurements. Inyl. J. Remote Sensing. 1999;20(2):225-40.
31. Paul F, Kääb A, Maisch M, Kellenberger T, Haeberli W. Rapid disintegration of Alpine glaciers observed with satellite data. Geophysical Research Letters. 2004; 31(21).
32. Dozier J. Spectral signature of alpine snow cover from the Landsat Thematic Mapper. Remote Sensing of Environment. 1989;28: 9-22.
33. Hall DK, Benson CS, Field WO. Changes of glaciers in Glacier Bay, Alaska, using ground and satellite measurements. Physical Geography. 1995;16(1):27-41.
34. Gupta RP, Haritashya UK, Singh P. Mapping dry/wet snow cover in the Indian Himalayas using IRS multispectral imagery. Remote Sensing of Environment. 2005;97(4):458-69.
35. Gratton DJ, Howarth PJ, Marceau DJ. Combining DEM parameters with Landsat MSS and TM imagery in a GIS for mountain glacier characterization. IEEE Transactions on Geoscience and Remote Sensing. 1990;28:766-9.
36. Wang J, Li W. Comparison of methods of snow cover mapping by analysing the solar spectrum of satellite remote sensing data in China. International Journal of Remote Sensing. 2003;24(21):4129-36.
37. Aniya M, Sato H, Naruse RE, Skvarca PE, Casassa G. The use of satellite and airborne imagery to inventory outlet glaciers of the Southern Patagonia Icefield, South America. Photogrammetric Engineering and Remote Sensing. 1996; 62(12):1361-9.
38. Andeson EA. A point energy and mass balance model of snow cover. NOAA Technical Report NWS 19, US Dept. of Commerce, National Weather Service; 1976.

39. Clark MP, Hendrikx J, Slater AG, Kavetski D, Anderson B, Cullen NJ, Kerr T, Örn Hreinsson E, Woods RA. Representing spatial variability of snow water equivalent in hydrologic and land-surface models: A review. Water Resour. Res. 2011;47(7).
40. Elder K, Rosenthal W, Davis RE. Estimating the spatial distribution of snow water equivalence in a montane watershed. Hydrological Processes. 1998; 12(1011):1793-808.
41. Machguth H, Eisen O, Paul F, Hoelzle M. Strong spatial variability of snow accumulation observed with helicopter-borne GPR on two adjacent Alpine glaciers. Geophysical research letters. 2006;33(13).
42. Watson FG, Anderson TN, Newman WB, Alexander SE, Garrott RA. Optimal sampling schemes for estimating mean snow water equivalents in stratified heterogeneous landscapes. J. Hydrol. 2006;328(3):432-52.